Lessons Learned from Electron Microscopy of Deformed Opalinus Clay

Ben Laurich[1(✉)], Janos L. Urai[1,2], Guillaume Desbois[2], Jop Klaver[2], Christian Vollmer[3], and Christophe Nussbaum[4]

[1] Federal Institute for Geosciences and Natural Resources (BGR), Stilleweg 2, 30655 Hannover, Germany
Ben.Laurich@bgr.de
[2] Structural Geology, Tectonics and Geomechanics, RWTH Aachen University, Lochnerstrasse 4-20, 52056 Aachen, Germany
[3] Institute for Mineralogy, University Münster, Correnstraße 24, 48149 Münster, Germany
[4] Swiss Geological Survey, Federal Office of Topography Swisstopo, Seftigenstrasse 264, 3084 Wabern, Switzerland

Abstract. Using a combined approach of ion-beam milling and electron microscopy, we observe, describe and quantify the microstructure of naturally and synthetically deformed Opalinus Clay (OPA) and deduce its microstructural evolution and underlying deformation mechanisms. The investigated samples derive from the so-called Main Fault, a 10 m offset fold-bend thrust fault crossing the Mont Terri Rock Laboratory in the Swiss Jura Mountains. The samples are slightly overconsolidated, experienced a burial depth of 1350 m and a maximum temperature of 55 °C. Most impact on strain is attributed to frictional sliding and rigid body rotation. However, trans-granular fracturing, dissolution-precipitation of calcite, clay particle neoformation and grain deformation by intracrystalline plasticity have a significant contribution to the fabric evolution. The long-term in-situ deformation behavior of OPA is inferred to be more viscous than measured at laboratory conditions.

Introduction

Several geoscience disciplines evaluate the suitability of the Opalinus Clay formation (OPA) to host a repository for nuclear waste. Most of them benefit from or even rely on insight of the OPAs' microstructure. In particular, hydro-mechanical studies profit from the understanding of microstructural processes. In this contribution, we present a summary of our results in observing, describing and quantifying the microstructure of naturally and synthetically deformed OPA (Laurich 2015; Laurich et al. 2016, Laurich et al. 2014). From this description, we further deduce the microstructural evolution from undeformed protolith to intensely deformed tectonite and aim to uncover underlying deformation mechanisms.

Rock fabric and rheological behavior depend on lithological and environmental controls (Rutter et al. 2001), both of which are fairly known for the well-researched OPA formation (e.g. Amann and Vogelhuber 2015; Clauer et al., accepted; Houben et al. 2013; Mazurek et al. 2006; Nussbaum et al. accepted). However, a comprehensive,

A. Ferrari and L. Laloui (eds.), *Advances in Laboratory Testing and Modelling of Soils and Shales (ATMSS)*, Springer Series in Geomechanics and Geoengineering,
DOI 10.1007/978-3-319-52773-4_40

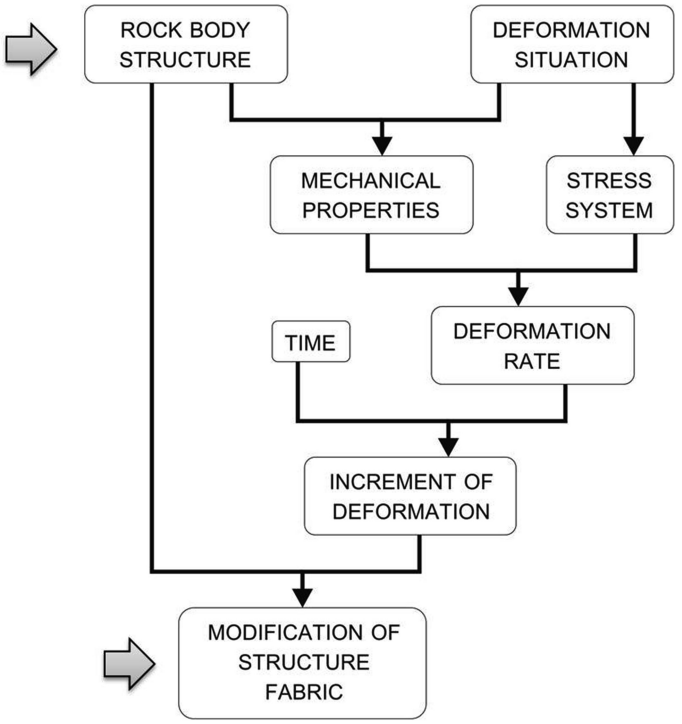

Fig. 1. General scheme of interacting factors that produce microstructural changes. Arrows point towards the factors that we optically examined, the remaining factors are intensely studied by other authors. Yet, a comprehensive, self-consistent model linking all elements is complex and missing. See text for details. Simplified after Hobbs et al. (1976).

self-consistent model on the deformation of OPA (Fig. 1) is missing, in particular for long-term in-situ deformation.

Using mostly electron microscopy techniques, we found five major deformation features in OPA from the Mont Terri Rock Laboratory: (1) slickensides, which are in cross-sectional view associated to (2) a μm-thin zone of slickenside-parallel oriented particles, (3) gouge, (4) calcite and celestite veins and (5) scaly clay.

Methods

All samples originate from the shaly facies of OPA from the Mont Terri Rock Laboratory (CH). They were retrieved either as outcrop or as drill core samples in vacuum sealed bags and got resin-stabilized in the laboratory. The samples were stored at dry conditions at room temperature. The wide majority of samples is from the so-called Main Fault, an up to 5 m wide fold-bend thrust fold with an offset in the rage of 10 m (Nussbaum et al. accepted).

Here presented results are obtained by: (1) Broad-Ion-Beam Scanning Electron Microscopy (BIB-SEM), JEOL SM09010 Ar-BIB, Zeiss Supra 55 SEM; (2) Focused-Ion-Beam Transmission Electron Microscopy (FIB-TEM), FEI Strata 205 FIB, Zeiss Libra 200FE.

The BIB (1) produces a smoothly polished (+/−5 nm surface roughness, Klaver et al. 2012) 2 mm^2 large surface free from mechanical polishing artifacts. Figure 2 illustrates the BIB-milling setup, where a combination of resin and cover glass minimizes any 'curtaining effects' by the BIB. The FIB (2) was conducted at samples with a thick W-coating (>50 nm) to preserve the structure directly underlying the sample surface. All procedures cut the samples parallel to shear direction and perpendicular to the faults' strike orientation (Fig. 2).

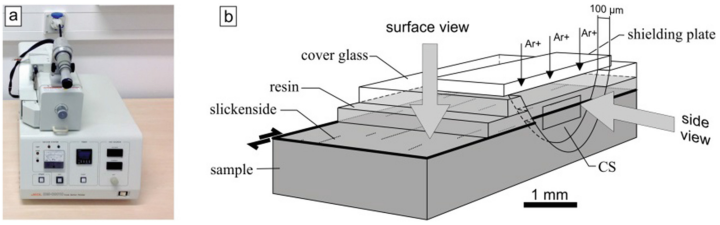

Fig. 2. (a) JEOL SM09010 Ar-BIB cross-section polisher, (b) Sketch of the BIB-milling setup from Laurich et al. (2014). CS = cross-section.

Results and Discussion

With a gentle force by hand, the samples from the Main Fault split perfectly along cohesionless slickensided surfaces, which show various types of kinematic indicators for frictional sliding (e.g. striae in Fig. 3a). An SEM-EDX map (Fig. 3b) illustrates Ca patches at slickenside risers, while Ca is scarce at restraining surfaces between. This Fig. 3 shows that despite cataclastic processes (e.g. frictional sliding), diffuse mass transport by pressure solution precipitation of calcite is an important deformation mechanism. This time-dependent mechanism cannot be easily reproduced at laboratory conditions (cf. Niemeijer et al. 2008).

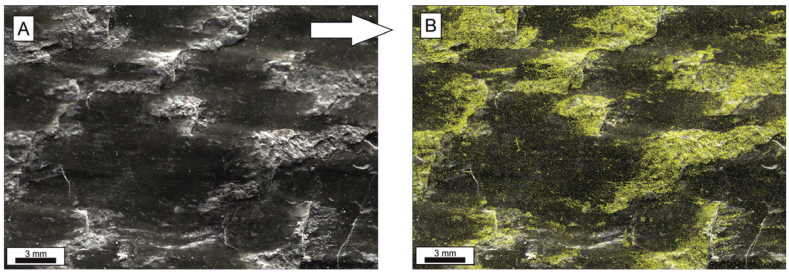

Fig. 3. Photograph (A) and SEM-EDX Ca distribution map of a slickensided surface from the Main Fault in the Mont Terri Rock Laboratory. Note that Ca patches correspond to brighter areas in the photograph, which are associated to risers (from Laurich 2015).

In side-view (Fig. 4), the slickensided surfaces are only a few microns wide, show a drastic loss in porosity, and nano-meter wide clay particles that enchase larger grains to build an absolutely flat surface. Figure 4a and b derive from the same FIB lamellae yet show indicators for different deformation mechanisms. (b) gives the impression of rigid body rotation, with larger grains wrapped by smeared clay particles and porosity in strain shadow regions. Contrary, (a) shows no porosity and strict face-to-face aligned larger minerals. This finding might be a product of clay neoformation as postulated

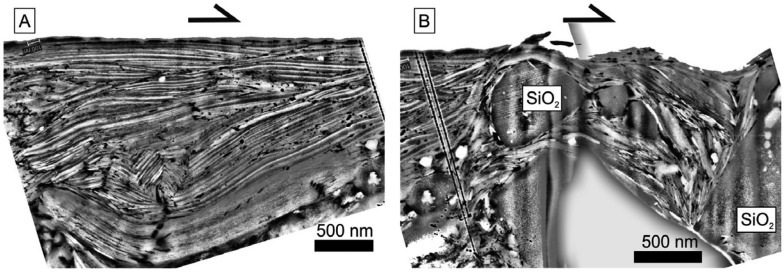

Fig. 4. TEM (HAADAF) images of an FIB lamella (from Laurich et al. 2014).

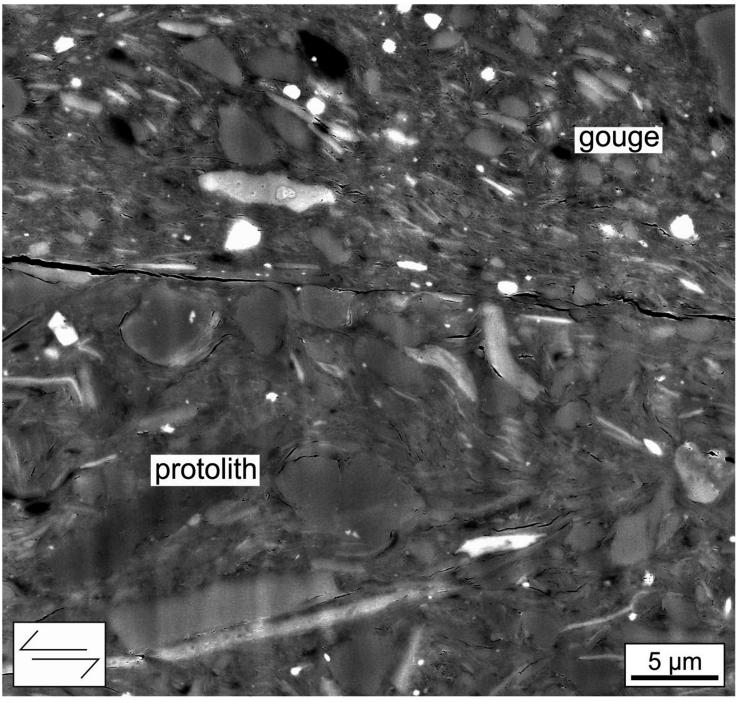

Fig. 5. BIB-SEM image of gouge next to protolith. Gouge and protolith are separated by a µm-thin shear zone that opened during sampling (black crack). Note the high fabric intensity in P-foliation and the grain size reduction for gouge.

elsewhere by geochemical analysis (Clauer et al. accepted; Warr et al. 2014) and/or a product of strong intracrystalline plasticity, both leaving no inter-grain porosity.

We interpret paleo fluid flow along but not perpendicular to the slickensides, which are μm-thin shear zones of sharp localized deformation: neighboring areas show the same microstructure as the undeformed protolith.

The μm-thin shear zone can be regarded as an elemental building block of other microtectonic features, such as gouge from the Main Fault. Figure 5 displays a μm-thin shear zone resembling a boundary of an gouge-internal shear band. Particles next to the shear zone are passively rotated into strict P-foliation, reduced in grain size, and frequently fractured. By EDX (not shown), gouge contains almost no calcite.

From our findings, we infer that gouge has a very low permeability, yet evolved from highly strained scaly clay by an abrasive dissolution process and deforms in a viscous manner with solid lubrication by nm-sized clay particles.

Conclusion and Relevance

We provide a microphysical basis to relate microstructures to macroscopic observations of strength and permeability. However, more work is necessary to link the factors in Fig. 1. We emphasize a strong collaboration of deformation testing and corresponding microstructural analysis in order to deduce the impact of each rheology controlling factor on the constitutive behavior of OPA.

Numerical modellers of long-term deformation behaviour of clays should not rely on laboratory derived parameters only, but implement more time-dependent processes to obtain realistic hydro-mechanical properties, resulting in a viscous long-term deformation. Our findings are also relevant to earthquake research, in particular to scaly clay fabrics in accretionary prisms.

References

Amann F, Vogelhuber M (2015) Expert Report - Assessment of Geomechanical Properties of Intact Opalinus Clay

Clauer N, Techer I, Nussbaum C, Laurich B (accepted) Geochemical signatures of paleofluids in calcite from microstructures and matrix of the main fault in the opalinus clay: a contribution to the regional evolutionary model. Swiss J Geosci

Hobbs B, Means W, Williams P (1976) An outline of structural geology. Wiley, New York

Houben ME, Desbois G, Urai JL (2013) Pore morphology and distribution in the shaly facies of opalinus clay (Mont Terri, Switzerland): insights from representative 2D BIB–SEM investigations on mm to nm scale. Appl Clay Sci 71:82–97. doi:10.1016/j.clay.2012.11.006

Klaver J, Desbois G, Urai JL, Littke R (2012) BIB-SEM study of the pore space morphology in early mature posidonia shale from the hills area. Germany Int J Coal Geol 103:12–25. doi: 10.1016/j.coal.2012.06.012

Laurich B (2015) Evolution of microstructure and porosity in faulted Opalinus Clay. RWTH-Aachen

Laurich B, Urai JL, Desbois G, Vollmer C, Nussbaum C (2014) Microstructural evolution of an incipient fault zone in opalinus clay: insights from an optical and electron microscopic study of ion-beam polished samples from the main fault in the mt-terri underground research laboratory. J Struct Geol 67:107–128. doi:10.1016/j.jsg.2014.07.014

Laurich B, Urai JL, Nussbaum C (2016) Microstructures and deformation mechanisms in opalinus clay: insights from scaly clay from the Main Fault in the Mont Terri Rock Laboratory (CH). Solid Earth Discuss, 1–30. doi:10.5194/se-2016-94

Mazurek M, Hurford AJ, Leu W (2006) Unravelling the multi-stage burial history of the Swiss Molasse Basin: integration of apatite fission track, vitrinite reflectance and biomarker isomerisation analysis. Basin Res 18:27–50. doi:10.1111/j.1365-2117.2006.00286.x

Niemeijer A, Marone C, Elsworth D (2008) Healing of simulated fault gouges aided by pressure solution: results from rock analogue experiments. J Geophys Res 113:B04204. doi:10.1029/2007JB005376

Nussbaum C, Kloppenburg A, Caer T, Bossart P (accepted) Tectonic evolution of the Mont Terri region, northwestern Swiss Jura: constraints from kinematic forward modelling. Swiss J Geosci

Rutter EH, Holdsworth RE, Knipe RJ (2001) The nature and tectonic significance of fault-zone weakening: an introduction. Geological Society, London, Special Publications, vol. 186, pp. 1–11. doi:10.1144/GSL.SP.2001.186.01.01

Warr LN, Wojatschke J, Carpenter BM, Marone C, Schleicher AM, van der Pluijm BA (2014) A "slice-and-view" (FIB–SEM) study of clay gouge from the SAFOD creeping section of the San Andreas fault at $\sim$2.7 km depth. J Struct Geol 69:234–244. doi:10.1016/j.jsg.2014.10.006